INFORME **DFN/RA-01/SP-26**

REF. EXTERNA

INERT MATRICES PREPARATION BY SOL-GEL (IONMAT PROJECT. SUBTASK 1.4)

DIVISIÓN DE FISIÓN NUCLEAR

Ciemat Centro de Investigaciones Energéticas, Medioambientales y Tecnológicas

TITULO: Inert matrices preparation by SOL-GEL (IONMAT project. Subtask 1.4)

AUTORES: A. Núñez; N. Rodríguez-Villagra, J.M. Elorrieta; A. Milena-Pérez; S. Fernández-Carretero; L. Gutiérrez; S. Durán; L. Anta; H. Galán

Zirconium–neodymium oxide microspheres were synthesized by the internal gelation (IG) sol–gel route. Aqueous nitrate solutions of Zr and Nd were gelled through the thermal decomposition of HMTA/urea in hot silicone oil, producing homogeneous spheres without powder handling. Process parameters—including metal concentration, HMTA/urea ratio, gelation temperature and washing protocol—were optimized to obtain stable microspheres containing 0–30 wt% Nd. Compositions with 50 wt% Nd did not gel under the explored conditions. The products were characterized by ICP-MS, TGA, SEM-EDX and XRD. Calcination at 600 °C ensured complete removal of organics and development of crystalline ZrO_2 with Nd uniformly distributed across the sphere radius. The washing step proved critical: TCE followed by dilute NH_4OH preserved surface integrity, whereas ethanol, acetone or concentrated ammonia induced degradation and Nd leaching. The resulting microspheres exhibit suitable size, homogeneity and dust-free handling characteristics, making them promising precursors for the fabrication of mixed $(Zr,U)O_2$ fuels for PCI simulation.

	NOMBRE	FIRMA	FECHA
Preparado por:	A. Núñez		
Revisado por:	N. Rodríguez-Villagra		
Conf por A. C.:	S. Fernández		
Aprobado por:	E.M. González		

FECHA DE EMISIÓN

INDEX

1. INTRODUCTION

Sol–gel routes have become highly attractive for the fabrication of advanced nuclear fuel materials owing to their ability to produce chemically homogeneous solids at relatively low temperatures while avoiding the handling of fine radioactive powders. Among these routes, the **internal gelation (IG)** process enables the formation of spherical particles with controlled size, high compositional uniformity and excellent flowability, features that are particularly valuable for the remote fabrication of minor-actinide-bearing fuels and targets [1, 2]. In IG, metal nitrate solutions are mixed with urea and hexamethylenetetramine (HMTA); the thermal decomposition of HMTA inside droplets generates ammonia *in situ*, inducing homogeneous precipitation and the formation of dense gel microspheres [3]. This approach minimises dust generation and allows an accurate control of stoichiometry at the molecular level.

Zirconia-based matrices have been investigated [4-10] as inert hosts for actinides because of their high melting point, chemical stability and low neutron absorption. Producing Zr–Nd microspheres by internal gelation also constitutes a relevant step towards the preparation of mixed $(Zr,U)O_2$ materials intended for the study of pellet–cladding interaction (PCI). The spherical geometry obtained by IG facilitates subsequent pressing and sintering while preserving a uniform distribution of the surrogate element within the matrix, a key requirement for reproducing the thermo-mechanical conditions expected in real fuels.

In this context, the present work aims to develop and optimise an IG-based sol-gel methodology (Figure 1) for the fabrication of Zr-doped oxide microspheres as a preliminary step (“cold stage”) towards the preparation of $(Zr,U)O_2$ model fuels. Particular attention is paid to the control of composition, microstructure and thermal behaviour, as these parameters govern the representativeness of the material for PCI simulation studies.

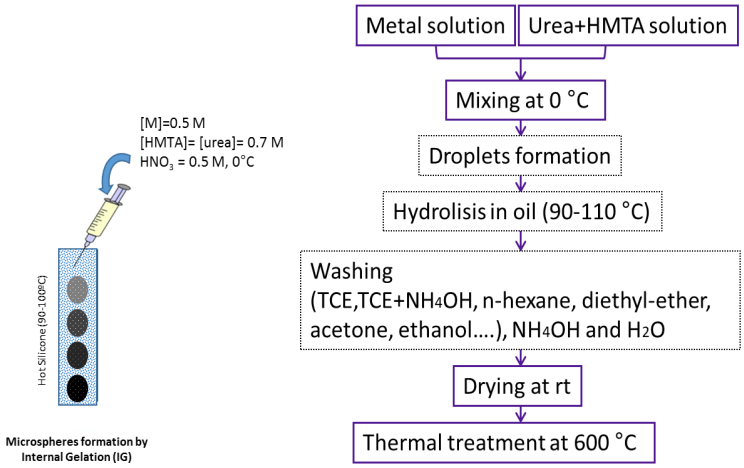

Figure 1. Flowsheet of microsphere formation by IG

In this preliminary study, we focus on the wet-route fabrication of Nd_2O_3-ZrO_2. ZrO_2 was used as the matrix because it will be part of the oxidized cladding. It should be noted that the formed solid has been aged, washed, filtered, dried, and finally calcined but not sintered, therefore, the addition of trivalent elements as Sc^{3+}, Y^{3+} or other rare-earths, usually used for ZrO_2 stabilization [11], was ignored here.

The microspheres are obtained by IG from aqueous nitrate solutions of Zr and Nd. Gelation is induced by the indirect generation of ammonia via the thermal decomposition of urea/HMTA, after the droplets are introduced into a column filled with hot silicone oil (90–100 °C), which acts as a heat carrier [9, 12]. The corresponding flowsheet is shown in Figure 1. Both the solutions and the resulting solids were analysed using the available techniques at CIEMAT (ICP-MS, TGA, SEM, XRD, Raman).

2. EXPERIMENTAL PROCEDURE. EQUIPMENT AND EXPERIMENTAL TECHNIQUES

2.1 REAGENTS AND SOLUTIONS

$ZrO(NO_3)_2 \cdot nH_2O$ salt (Acros Organics, 99.5%) was dissolved in deionised water at room temperature. Nd was introduced as $Nd(NO_3)_3 \cdot 6H_2O$ (Thermo Scientific, 99.5%) dissolved in HNO_3 solution to obtain a final and constant total metal concentration of 0.5 mol/L [13, 14]. The targeted molar composition in the final oxide of (100:0), (97:3), (95:5), (90:10), (70:30), (50:50) wt% Zr-Nd hereafter referred to as 0, 3, 5, 10, 30 and 50 wt% Nd. A second solution was prepared by dissolving constant concentrations of urea (Thermo Scientific, 99.5%) and hexamethylentetramine (HMTA, Alfa Aesar, 99+%), in deionised water. The metal solution (Zr+Nd, 2.0 mL) was stirred in an ice bath and a precooled solution (2.0 mL) containing HMTA (1.4 mol/L) and urea (1.4 mol/L) was added, leading to c(M=Zr+Nd) = 0.5 mol/L and R = 1.4 for both gelation agents. The relative molar concentrations of urea and HMTA with respect to the total metal concentration were defined by the two molar ratios: R_u = [urea]/[metal] (mol/mol) and R_H = [HMTA]/[metal] (mol/mol), where metal represents the sum of metallic cations.

The washing agents employed to remove silicone oil were used as received: 1,1,2,2 tetrachloroetane (TCE) (Fluka, ≥ 98%), n-hexane (Merck, for analysis), diethylether (Panreac, stabilized 6 ppm BHT, PRS), ethanol (Merck, absolute for analysis) and acetone (Panreac, PRS). The NH_4OH solution (Merck, ammonia solution for analysis 25%) was diluted in MQ water to 0.1 mol/L.

2.2 TECHNIQUES

The main characterization techniques that have been used for the analysis of the samples are summarized below (see Table 1).

Table 1. Methods and techniques used in this project

Technique	Parameter	Equipment
ICP-MS	Elemental identification (quantification).	Thermo Fischer Scientific iCAP™ Q with collision cell technology.
TGA	Thermal behaviour up to 900 °C (10 °C·min^{-1}, 60 mL·min^{-1} air).	TGA Q50 thermobalance (TA Instruments, V20.13 Build 39).
Oven	Drying of the precipitated samples at 135-200 °C, 24 h.	Memmert VO 200-29L, Vacuum Oven.
Muffle furnace	Calcination at 600-700 °C for 1 h under air flow, heating rate from 2.5, 5 and 10 °C/min.	Ney 6-525 programmable furnace.
SEM-EDX	Surface morphology, grain size, elemental identification (semiquantification).	HITACHI TM4000 Plus (15 kV).
XRD	Phase identification, lattice parameters.	Bruker D8 ADVANCE Eco; Cu Kα radiation (λ=1.54056 Å), 40 kV, 25 mA. Bragg-Brentano configuration geometry. Software: EVA and TOPAS[1] (Bruker Analytical X-Ray Systems).

The efficiency of the washing step was assessed by Inductively Coupled Plasma - Mass Spectrometry (ICP-MS) analysis of the effluent before and after precipitation. Zr and Nd concentrations in the initial solutions were determined using Thermo Fischer Scientific iCAP™ Q ICP-MS equipped with collision cell technology. Aqueous samples were analysed directly after appropriate dilution with HNO_3 (2–5% v/v).

The thermal behaviour of the microspheres during heating in air from room temperature to 900 °C was investigated by thermogravimetric analysis (TGA). Measurements were performed using a TGA Q50 thermobalance (TA Instruments, V20.13 Build 39) with a heating rate of 10 °C/min up to 900 °C under a synthetic air flow at 60 mL/min. A pure nitrogen flow of 40 mL/min was used as a balance purge gas. Calibration of the TGA was performed using magnetic standards (Curie point, ASTM 1582) of Alumel and Ni (153 and 358 °C, respectively), and weight (200 mg – 1 g weight range). Oxidation tests were conducted in an open platinum crucible from room temperature up to 700 °C at

[1] EVA is used for phase identification through comparison with crystallographic databases, and TOPAS is for quantitative phase analysis and structural refinement based on profile fitting methods.

10 °C/min, to obtain the complete conversion to ZrO_2-Nd_2O_3 and to evaluate the overall reaction. Thermogravimetric curves were processed using the software *Universal Analysis* (TA Instruments).

The microspheres were dried in air overnight at room temperature and subsequently heated in an oven at 135 °C for 24 h to remove interstitial water (Memmert VO 200-29L, Vacuum Oven). The temperature was then increased to 200 °C. Calcination was then performed at 600 °C for 1 h under air flow with different heating rates from 2.5 °C/min, 5 °C/min and 10 °C/min in a Ney 6-525 Programmable muffle furnace. An intermediate heating rate was selected as a compromise to ensure adequate material properties while maintaining a reasonable processing time.

Sample surface morphology was examined using a Scanning Electron Microscopy Energy Dispersive X-ray spectroscopy (SEM EDX) HITACHI TM4000 Plus SEM at 15 kV and coupled with an energy-dispersive X-ray analyser (EDX, QUANTAX 75 / 80 Microanalysis Systems for Hitachi Microscopes).

Crystalline structure and phase composition were analysed by X-Ray Diffraction (XRD, Bruker D8 Advance Eco diffractometer) at room temperature using Cu $K\alpha_1$ radiation (λ= 1.540598 Å) in a Bragg-Brentano geometry, operating at 40 kV and 25 mA. Data processing and lattice parameter refinement were carried out using TOPAS software (Bruker).

Raman spectroscopy was also attempted; however, reliable spectra could not be obtained, most likely due to the nanocrystalline nature of the samples, which generated a strong fluorescence background.

3. RESULTS

In the present work, Zr–Nd microspheres were prepared by IG from a cold aqueous nitrate solution containing Zr and Nd. Gelation was induced by indirect ammonia generation through the thermal decomposition of urea and HMTA. The solution was dispensed dropwise using a syringe and hollow needle into a glass column filled with silicone oil maintained at 90-110 °C, which acted as a heat carrier [12, 15]. Upon heating, HMTA decomposes with temperature, leading to a gradual increase in pH of the solution, and subsequent gel formation according to Eqs. (1) and (2) [15, 16]:

$$(CH_2)_6N_4 + HNO_3 \rightarrow [(CH_2)_6N_4H]NO_3 \quad (1)$$

$$[(CH_2)_6N_4H]\,NO_3 + 3HNO_3 + 6H_2O \rightarrow 4NH_4NO_3 + 6CH_2O \quad (2)$$

The ammonia generated promotes the precipitation of the metal hydroxides, resulting in a homogeneous gel network, as illustrated in Eqs. (3) and (4):

$$[Zr_4(OH)_8(OH_2)_{16}]X_8 + 8H_2O \rightarrow [Zr_4(OH)_{16}\,16H_2O] + 8HX \quad (X=Cl^-/NO_3^-) \quad (3)$$

$$Nd(NO_3)_3 + 3NH_4OH \rightarrow Nd(OH)_3 + 3NH_4NO_3 \quad (4)$$

The concentrations of urea, HMTA, metal ions and HNO_3 were slightly optimized (Figure 2) based on previously published data, maintaining a ratio [urea]/[HMTA] = 1.0 within the ranges 0.7–3.6 mol/L for both gelation agents, 0.2–4.5 mol/L for HNO_3 and 0.5-1.5 mol/L for total metal concentration [15, 17, 18].

The Zr/Nd ratios were adjusted to obtain oxides containing 0, 3, 5, 10, 30 and 50 wt% Nd, fixing the final metal concentration at 0.5 mol/L in diluted nitric acid (Figure 2). A second solution with constant concentrations of urea and HMTA in cold deionised water was prepared at 0 °C[2] and introduced into the hot silicone oil column in two batches of about 2 mL; the complete addition required less than 5 min. Gelation was not achieved at the highest Nd content (50 wt%), indicating limitations of the process at high trivalent cation concentrations.

[2] To prevent a premature gelation, the solution is cooled down to a temperature between 0 °C and 5 °C before the experiment.

After gelation, microspheres were aged, filtered, and washed with different washing agents and diluted NH_4OH/H_2O, followed by drying and calcination at 600 °C in air. The resulting materials were characterized by the techniques described in section 2.2.

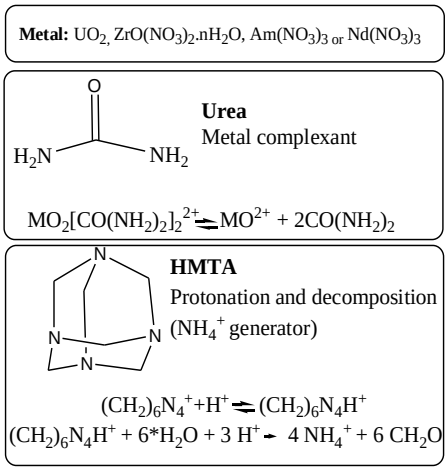

	Concentrations in mol/L
[Metal]=[Zr]+[Nd]	0.5-1.5
[urea]=[HMTA]	0.7-3.6
[HNO_3]	0.2-4.5

Figure 2. Range of concentrations of metals and complexing agents employed and different parameters studied in these experiments

Extensive optimisation of the IG parameters for the ZrO_2-Nd_2O_3 microspheres fabrication was performed, including column design, silicone oil temperature, reagent concentrations, needle diameter, washing protocol and oven tray configuration. Although 90–100 °C is commonly recommended for gelation, improved sphericity and mechanical stability were obtained at 110 °C (Figure 3).

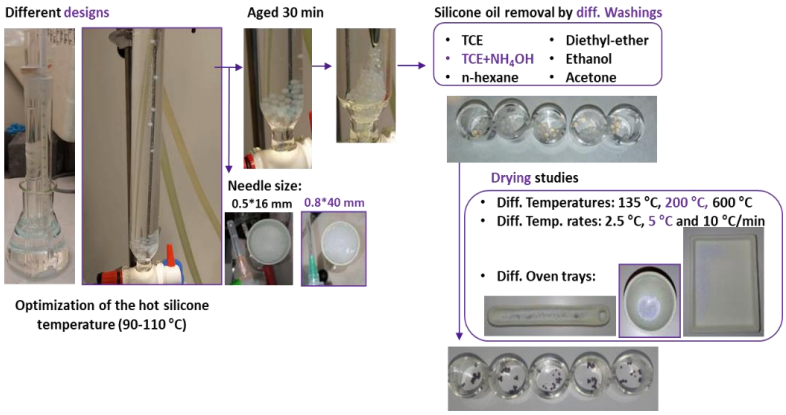

Figure 3. Experimental setup for the internal gelation process to obtain ZrO_2-Nd_2O_3 microspheres

After completion of droplet addition, heating was switched off and the gelled droplets were removed from the column when the oil temperature had decreased to approximately 40 °C (20-30 min). Following washing, the spheres exhibited a pure white color typical of Zr(IV); increasing Nd(III) content progressively shifted the color towards bluish–purple tones [19][3]. The microspheres were collected by Büchner filtration, and several washing agents reported in literature were evaluated: tetrachloroethane (TCE), TCE followed by 0.1 mol/L of NH_4OH, n-hexane, diethyl-ether, ethanol or acetone [13, 14, 20, 21].

When the microspheres were washed with ethanol or acetone (Figure 4a) noticeable surface leaching and degradation was observed. Such behaviour was not reported for systems based on cerium or uranium [18], suggesting a specific sensitivity of Zr–Nd gels. In agreement with Collins *et al*. [18], the use of concentrated NH_4OH led to partial redissolution, particularly of Nd, as confirmed by ICP-MS analysis of the washing solutions with NH_4OH (Figure 4b). Consequently, cold and dilute ammonia solutions are recommended to minimise unwanted solubilization.

[3] The sharp absorption bands of neodymium cause the glass color to change under different lighting conditions, being reddish-purple under daylight or yellow incandescent light, but blue under white fluorescent lighting, or greenish under trichromatic lighting.

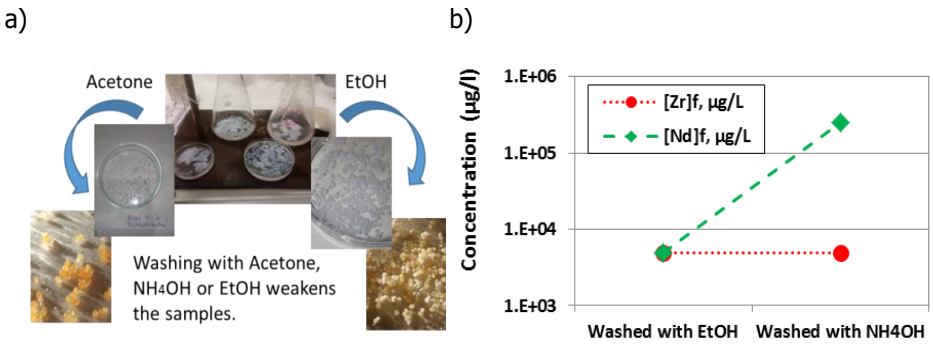

Figure 4: a) The erosion produced when the microspheres were cleaned with ethanol or acetone. And b) the ICP-MS analysis of the supernatant after the washing step with ethanol or NH_4OH

A systematic ICP-MS comparison of the washing agents was not carried out because their very different chemical matrices could induce substantial matrix effects, leading to errors potentially greater than the measured concentrations. Visual inspection and SEM observations indicated that only ethanol, acetone and concentrated NH_4OH caused significant degradation.

Thermogravimetric analysis of the precursor reagents indicated that the main mass losses take place below 600 °C, after which the mass remains essentially constant. (Figure 5). Benay et al. [11] reported endothermic events peaks at 124, 172 and 253 °C, which can be related to the melting of urea and the decomposition stages [22, 23]. A large exothermic peak was then observed at 352 °C, corresponding to reactions between the decomposition products of HMTA and urea. Our results are consistent with these observations.

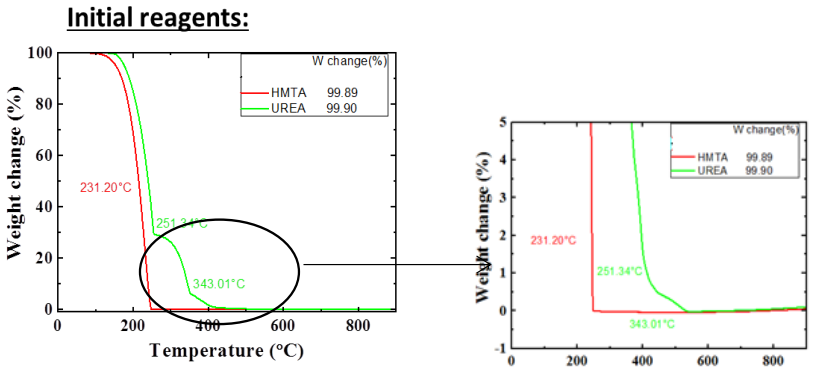

Figure 5. TGA analysis and extension of the temperature range of interest of urea and HMTA, the initial reagents used in IG

TGA of the IG-derived solids (Figure 6) revealed that increasing the proportion of Nd reduced the overall mass loss. Curves are plotted from 150 °C onwards because there have been different thermal pre-treatments (135-200 °C). The main weight loss occurred between 260 and 300 °C. The exothermic effect at 405 °C reported in the literature [11], attributed to the decomposition of the silicone oil remaining on the surface of the spheres, was not observed, indicating efficient washing.

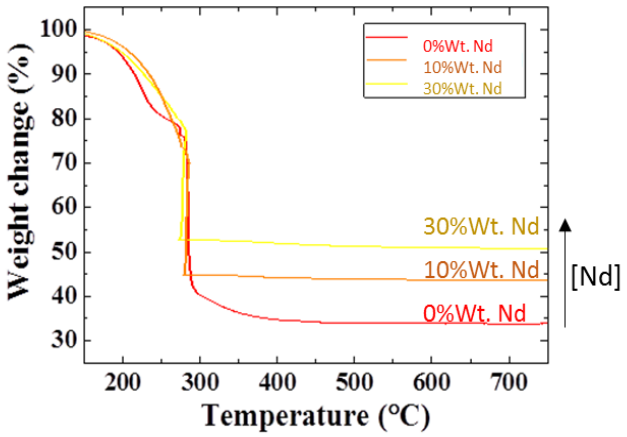

Figure 6. TGA of some representative Zr-Nd samples obtained by IG

Finally, after washing, the microspheres were overnight dried in air at room temperature, placed in an oven at 135 °C, and then calcined in air at 600 °C for 1 h (at different heating rates: 2.5, 5 and 10 °C/min) in order to avoid microsphere surface cracking. The analysis of the morphological structure by SEM showed that a temperature of 135 °C (which appeared sufficient to remove H_2O) was insufficient to remove residual urea and HMTA located around the microsphere (Figure 7); increasing the temperature to 200 °C eliminated these residues.

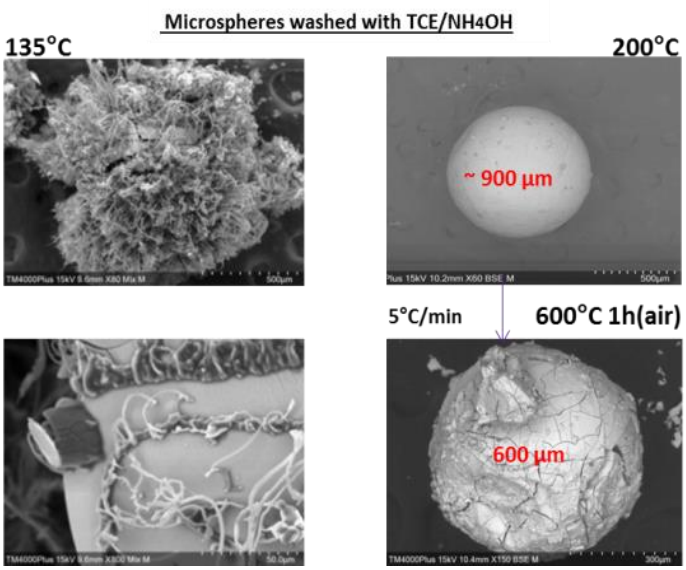

Figure 7. SEM of microspheres obtained by IG dried at 135 °C and 200 °C

The dimensions obtained here (Figure 7 and Figure 8) satisfy the requirements for remote handling and subsequent pelletization [24].

Among the washing agents tested, TCE followed by diluted NH_4OH produced the cleanest surfaces (Figure 8). As visually observed (Figure 4) and according to literature [15, 23], cleaning with acetone, ethanol or NH_4OH produced leaching, erosion and weakening of the microsphere surface.

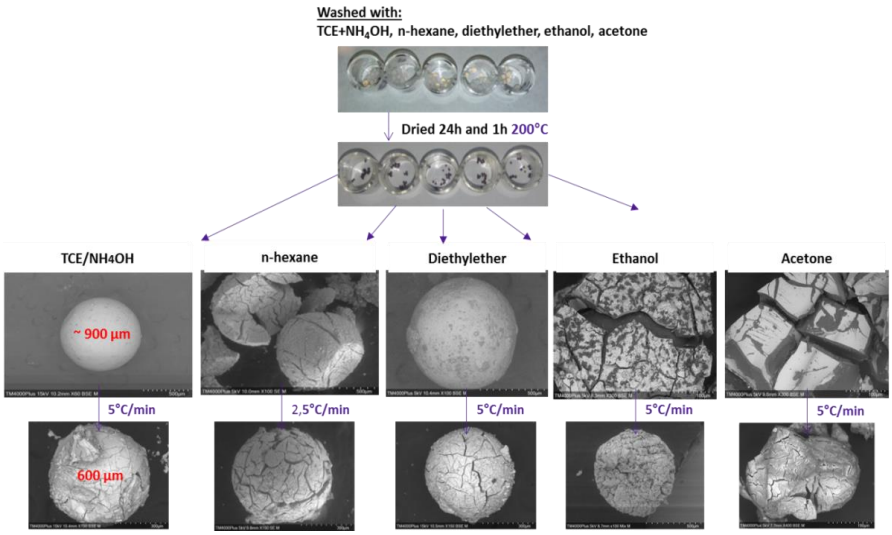

Figure 8. SEM images of microspheres after different washing procedures

EDX line scans performed on fractured spheres confirmed a highly homogeneous distribution of Nd from the core to the surface (Figure 9), demonstrating the intrinsic compositional uniformity achieved by IG.

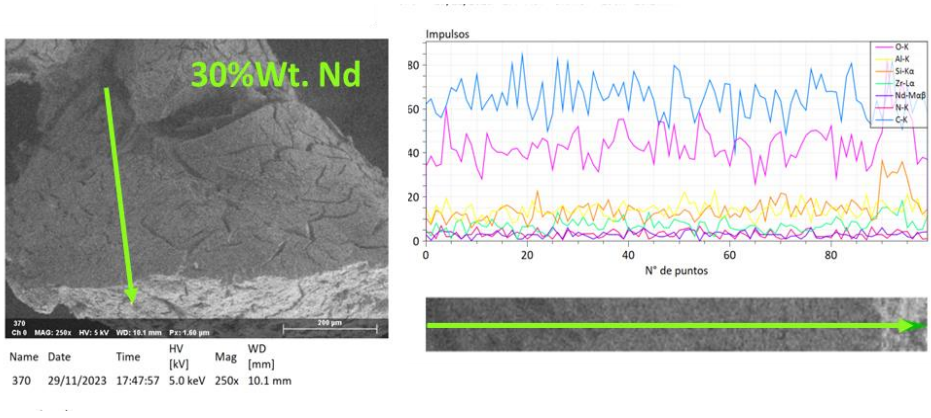

Figure 9. SEM-EDX profile across a 30 wt% Nd microsphere washed with TCE and NH_4OH after calcination

Pure zirconia naturally exhibits a monoclinic (m) structure at room temperature, transforming to a tetragonal (t) form at about 1170 °C and then to a cubic (c) fluorite structure around 2370 °C (Figure 10), with melting at 2716 °C [7, 22]. These martensitic transformations involve significant volume changes (≈2.3% for c→t and ≈4.5% for t→m),

which cause fragmentation upon cooling unless stabilized by dopants [25-29]. Similar phase stability considerations in zirconia-based systems have also been discussed in the internal DFN report in the context of U–Zr materials [30].

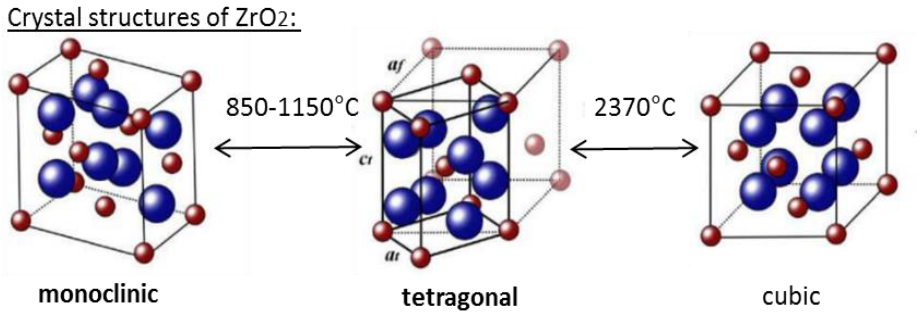

Figure 10. Crystal structures of ZrO_2 [31]

Building on the established understanding of zirconia's phase transformations and stabilization mechanisms [7], XRD analyses performed after different thermal treatments demonstrated a clear increase in crystallinity with temperature (Figure 11). The refined lattice parameter obtained (a = 5.5455 Å) differs from the reference value (5.16658 Å, reference code 96-210-0389) published in the literature [32, 33], reflecting Nd incorporation and nanoscale effects. Peak broadening indicated progressive crystallite growth up to 600 °C, in agreement with published data [5, 23, 33]. No reflections corresponding to Nd_2O_3 were detected, suggesting that Nd was incorporated into the ZrO_2 lattice and consequently the absence of segregated phases.

Raman spectroscopy could not provide reliable information due to the strong fluorescence background typical of nanocrystalline zirconia.

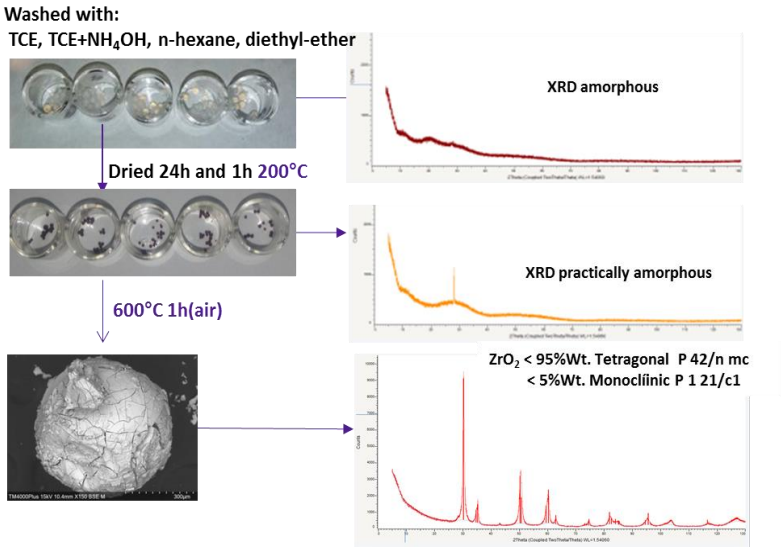

Figure 11. XRD patterns of the Zr-Nd microspheres obtained by IG after thermal treatments

4. CONCLUSIONS

Extensive optimisation of parameters for the internal gelation methodology has enabled the successful synthesis of zirconium-based oxide microspheres with controlled composition and microstructure. The key processing parameters, including reagent concentrations, gelation temperature, droplet formation and washing protocols, were precisely adjusted, allowing the homogeneous incorporation of actinides in the range 0–30 wt%. Compositions containing 50 wt% actinide could not be produced under the present conditions due to the absence of gelation, indicating a practical limit of the IG route for highly loaded trivalent systems.

The washing protocol was identified as a critical step. Cleaning with TCE followed by diluted NH_4OH yielded the best surface quality, whereas ethanol, acetone and concentrated ammonia caused degradation and partial re-dissolution, particularly of actinides. The resulting microspheres exhibited sizes and mechanical integrity compatible with dust-free handling and subsequent pellet pressing.

The different characterization techniques applied (SEM-EDX, TGA, and XRD) provided consistent and complementary information. Thermal treatments up to 600 °C significantly enhanced the crystallinity of the microspheres, while SEM-EDX analyses confirmed a uniform radial distribution of actinides, demonstrating the intrinsic chemical homogeneity achieved by IG. TGA results showed a systematic decrease in mass loss with increasing actinides content and confirmed that calcination at 600 °C is sufficient to obtain fully oxidized ZrO_2–actinides materials. XRD analyses indicated the formation of zirconia with increasing crystallite size after heat treatment, without detectable secondary actinide-rich phases, suggesting complete incorporation of actinides into the ZrO_2 lattice. These features make the produced materials suitable precursors for the preparation of mixed $(Zr,U)O_2$ systems aimed at simulating pellet–cladding interaction (PCI).

In general, the IG route is a robust and reproducible method for producing homogeneous Zr-based microspheres relevant to advanced nuclear fuel development. Optimal processing conditions were established for compositions up to 30 wt% actinide, providing a reliable surrogate route. Calcination at 600 °C ensures adequate removal of organics and development of crystalline structure.

Future work should focus on extending the methodology to uranium-containing systems to fabricate representative $(Zr,U)O_2$ materials and evaluating sintering behaviour and pellet fabrication from the microspheres.

5. REFERENCES

[1] D. Sood, "The role sol–gel process for nuclear fuels-an overview," *Journal of sol-gel Science and Technology,* vol. 59, pp. 404-416, 2011.

[2] G. Colak, G. Leinders, N. Vanhove, T. Mai, M. Verwerft, and J. Vleugels, "Fabrication of americium containing transmutation targets," *Journal of Nuclear Materials,* vol. 597, p. 155107, 2024.

[3] S. Uygur, R. Delville, C. Schreinemachers, G. Leinders, N. Vanhove, W. Van Renterghem*, et al.*, "Cation-heterogeneity in internally gelated $U_{1-z}Ce_zO_{2-x}$, 0.15≤ z≤ 0.3 microspheres," *Journal of Nuclear Materials,* vol. 587, p. 154749, 2023.

[4] R. C. Ewing, "Nuclear waste forms for actinides," *Proc Natl Acad Sci U S A,* vol. 96, pp. 3432-9, 1999.

[5] S. Fabris, A. T. Paxton, and M. W. Finnis, "A stabilization mechanism of zirconia based on oxygen vacancies only," *Acta Materialia,* vol. 50, pp. 5171-5178, 2002.

[6] R. C. Garvie and P. S. Nicholson, "Structure and thermomechanical properties of partially stabilized zirconia in the CaO-ZrO_2 system," *Journal of the American Ceramic Society,* vol. 55, pp. 152-157, 1972.

[7] J. P. Goff, W. Hayes, S. Hull, M. T. Hutchings, and K. N. Clausen, "Defect structure of yttria-stabilized zirconia and its influence on the ionic conductivity at elevated temperatures," *Physical Review B,* vol. 59, pp. 14202-14219, 1999.

[8] R. H. J. Hannink, P. M. Kelly, and B. C. Muddle, "Transformation toughening in zirconia-containing ceramics," *Journal of the American Ceramic Society,* vol. 83, pp. 461-487, 2000.

[9] C. Hellwig, M. Pouchon, R. Restani, F. Ingold, and G. Bart, "Fabrication and microstructure characterization of inert matrix fuel based on yttria stabilized zirconia," *Journal of Nuclear Materials,* vol. 340, pp. 163-170, 2005.

[10] Kinga Suchorab, Marcin Brykała, Magdalena Gawęda, Maciej Zieliński, Ryszard Diduszko, Kamil Kaszyca*, et al.*, "Structural investigation of sintered zirconia ceramics for nuclear applications-effects of Ce/Nd dopants and synthesis methods.," *Journal of Molecular Structure,* vol. 1349, p. 143911, 2026.

[11] G. Benay, F. Hubert, and G. Modolo, "Preparation of yttria-stabilized zirconia-ceria kernels as fuel precursors using internal gelation," *Radiochimica Acta,* vol. 96, pp. 285-291, 2008.

[12] C. Schreinemachers, G. Leinders, G. Modolo, M. Verwerft, K. Binnemans, and T. Cardinaels, "The conversion of ammonium uranate prepared via sol-gel synthesis into uranium oxides," *Nuclear Engineering and Technology,* vol. 52, pp. 1013-1021, 2020.

[13] G. Benay, "Fabrication of zirconia based ceramics by internal gelation for conversion of trivalent actinides.," Jülich Forschungszentrum Jülich GmbH Zentralbibliothek, Verlag, 2008.

[14] J. A. Katalenich, B. B. Kitchen, and B. D. Pierson, "Production of monodisperse cerium oxide microspheres with diameters near 100 µm by internal-gelation sol–gel methods," *Journal of Sol-Gel Science and Technology,* vol. 86, pp. 329-342, 2018.

[15] C. Schreinemachers, G. Leinders, G. Modolo, M. Verwerft, K. Binnemans, and T. Cardinaels, "Fabrication of Nd- and Ce-doped uranium dioxide microspheres via internal gelation," *Journal of Nuclear Materials,* vol. 535, p. 152128, 2020.

[16] J. L. Collins, M. H. Lloyd, and R. L. Fellows, "The basic chemistry involved in the internal-gelation method of precipitating uranium as determined by pH measurements," vol. 42, pp. 121-134, 1987.

[17] J. L. Collins, "Method for preparing hydrous zirconium oxide gels and spherules," Oak Ridge National Laboratory (ORNL), Oak Ridge, TN (United States) 2003.

[18] J. L. Collins, M. Lloyd, and S. E. Shell, "Control of urania crystallite size by HMTA–urea reactions in the internal gelation process for preparing (U, Pu)O_2 fuel kernels," *ORNL report ORNL/TM/10,* 2005.

[19] M. R. Ganjali, V. K. Gupta, F. Faridbod, and P. Norouzi, *Lanthanides series determination by various analytical methods*: Elsevier, 2016.

[20] M. Brykala, R. Walczak, D. Wawszczak, S. Kilim, M. Rogowski, E. Strugalska-Gola*, et al.*, "Preparation by the double extraction process with preliminary neutron irradiation of yttria or calcia stabilised cubic zirconium dioxide microspheres," *Nuclear Engineering and Technology,* vol. 53, pp. 188-198, 2021.

[21] G. Ledergerber, "Internal Gelation for Oxide and Nitride Particles " Japan Atomic Energy Research Inst., Tokyo (Japan)1996.

[22] P. M. Schaber, J. Colson, S. Higgins, D. Thielen, B. Anspach, and J. Brauer, "Thermal decomposition (pyrolysis) of urea in an open reaction vessel," *Thermochimica Acta,* vol. 424, pp. 131-142, 2004.

[23] E. C. Subbarao, *Science and technology of zirconia. Zirconia-an overview.* vol. ISSN 0730-9546. Columbus, OH, 1981.

[24] V. Anastasov, M. Betti, F. Boisson, F. Depisch, F. Houlbreque, R. Jeffree*, et al.*, "Status of minor actinide fuel development," *IAEA Nuclear energy series,* 2009.

[25] A. G. Evans and A. H. Heuer, "REVIEW—Transformation Toughening in Ceramics: Martensitic Transformations in Crack-Tip Stress Fields," *Journal of the American Ceramic Society,* vol. 63, pp. 241-248, 1980.

[26] K. Sato, H. Abe, and S. Ohara, "Selective Growth of Monoclinic and Tetragonal Zirconia Nanocrystals," *Journal of the American Chemical Society,* vol. 132, pp. 2538-2539, 2010.

[27] G. Skandan, H. Hahn, M. Roddy, and W. R. Cannon, "Ultrafine-Grained Dense Monoclinic and Tetragonal Zirconia," *Journal of the American Ceramic Society,* vol. 77, pp. 1706-1710, 1994.

[28] P. R. Rauta, P. Manivasakan, V. Rajendran, B. B. Sahu, B. K. Panda, and P. Mohapatra, "Phase transformation of ZrO2 nanoparticles produced from zircon," *Phase Transitions,* vol. 85, pp. 13-26, 2012.

[29] S. Vasanthavel and S. Kannan, "Structural investigations on the tetragonal to cubic phase transformations in zirconia induced by progressive yttrium additions," *Journal of Physics and Chemistry of Solids,* vol. 112, pp. 100-105, 2018.

[30] N. Rodríguez-Villagra, J. M. Elorrieta;, A. Milena-Pérez;, S. Fernández-Carretero;, A. Nuñez;, L. J. Bonales;*, et al.*, "DFN/RA-05/SP-24 Production and characterization of irradiated nuclear fuel surrogates by dry powder method (IONMAT project. Subtask 1.1)." 2024.

[31] J. A. M. Tabares, "Una visión general de los cerámicos de circona–estructura, propiedades y aplicaciones," *Revista Colombiana de materiales,* 2012.

[32] M. Yashima and S. Tsunekawa, "Structures and the oxygen deficiency of tetragonal and monoclinic zirconium oxide nanoparticles," *Acta Crystallographica Section B,* vol. 62, pp. 161-164, 2006.

[33] S. Limbu, "Investigation of crystal structure confinement and optical attributes of monoclinic–tetragonal Zirconia nanocrystals via chemical co-precipitation technique," *Bulletin of Materials Science,* vol. 45, p. 182, 2022.

FIRMANTE	NOMBRE	FECHA	NOTAS
FIRMANTE[1]	**ANA NUÑEZ GOMEZ-ALEIXANDRE**	**09/06/2026 11:48 | Sin acción específica**	
FIRMANTE[2]	**MARIA NIEVES RODRIGUEZ VILLAGRA**	**09/06/2026 13:40 | Sin acción específica**	
FIRMANTE[3]	**M.SOLEDAD FERNANDEZ FERNANDEZ**	**12/06/2026 08:04 | Sin acción específica**	
FIRMANTE[4]	**ENRIQUE MIGUEL GONZALEZ ROMERO**	**12/06/2026 12:30 | Sin acción específica**	